Online Trained Neural Network-PI Speed Controller for DTC based IPMSM Drives

Zhenyu Jia and Byeongwoo Kim
School of Electrical Engineering, University of Ulsan, Ulsan, South Korea
Email: hellojrain@gmail.com; bywokim@ulsan.ac.kr

***Abstract*—The paper presents an online trained NN-PI (Neural Network-Proportional Integral) speed controller employed in a SVM-DTC (Space Vector Modulation-Direct-Torque-Control) based Interior Permanent Magnet Synchronous Motor (IPMSM) drives. Back propagation (BP) algorithm is applied in training process to tune the parameters of PI speed controller. The proposed control method has been tested in simulation. Simulation results demonstrate that SVM-DTC scheme combined with the proposed NN-PI speed controller can improve performance with very fast speed response, smaller overshoot, robustness and low ripples in flux linkage and torque .**

***Index Terms*—neural network, back propagation algorithm, PI controller, SVM-DTC, IPMSM**

I. Introduction

Permanent magnet synchronous motors (PMSM) have been widely used in high-performance industrial drives. PMSMs have many advantages, such as high efficiency and power density, high torque-to-inertia ratio and simple structure. Inherent coupled flux and torque is the main disadvantage of PMSMs, which makes them hard to control. Many advanced control techniques have been presented to make PMSMs more comparable. Filed-oriented control (FOC) [1] and direct torque control (DTC) [2] are the two main control techniques for PMSM drives. The FOC technique is widely used in PMSM drives. However, it performs not as well as predicted in practical engineering application due to the variations of motor parameters and inaccurate control mode [3]. In 1980s, DTC algorithm [4] was firstly introduced from ABB for induction motor drives. Decades past, it was already developed and used for variety of motor drives.

Compared with FOC, DTC is a significantly new concept. It has many characteristics of less dependence on machine parameters, fast dynamic response and less complexity without coordinate transformation or current regulation [5]. Furthermore, it doesn't need extra sensors to implement DTC.

Although DTC possesses many advantages, it still has some shortages as reported in literatures [6]-[9]. First, the ripples in torque and flux are relatively high. Moreover, conventional DTC usually adopts a PI speed controller in the outer loop. Consequently, it usually causes improper speed transient response with high overshoot at the motor start stage, big speed ripples when system variations occur.

To solve the aforementioned problems of conventional DTC, varieties of optimization methods have been presented in [7]-[10]. Many of them can obtain better results in ripple reduction and fixed switching frequency. As reported in [8], the ripples are reduced by using multi-level converter which has more voltage space vectors. However, it needs more power switches thus increasing the system cost and complexity. In [9], a smoother torque can be expected. However, it adopts four controllers to control flux and torque which increases computational burden. A method combining modified DTC and SVM for PMSM was investigated in [7] and [10]. However, both of them apply PI speed controller which suffers some speed transient response problems.

Speed controller, usually been neglected, also plays an important role in DTC technique for PMSM drives. A PI controller is widely applied to in the outer speed regulator loop due to its relative simple implementation and effectiveness [11]. However, the PI control approach cannot perform sufficiently well in nonlinear PMSM drives system with various uncertainties [13]. Moreover, it is time consuming and hard to tune the proportional and integral gain parameters of PI controller. Recently, some new methods have been proposed to replace PI speed controller [12]-[14]. In [12], a neural speed controller was designed and adopted to improve the control performances of PMSM with FOC technique. In [13], artificial neural network (ANN) based on Kalman filter (KF) was used as speed controller. Although it can get better simulation results than conventional PI speed controller, it is relatively more complex by combining ANN and KF. Moreover, it lacks rapidity and stability compared with PI controller.

In this paper, a novel adaptive speed controller based on neural network PI (NN-PI) is presented. Neural network, which has the ability of approaching to any nonlinear systems with uncertainties, is applied to tune PI parameters, k_p and k_i [15]. Furthermore, a modified DTC based on SVM for IPMSM is adopted, which is similar to the schemes proposed in [7] and [10]. Effective DTC control for IPMSM drives can be obtained by using self-adaptive NN-PI controller and SVM. Simulation results demonstrate that proposed NN-PI speed controller combining SVM can enhance the operating performance with faster transient response, smaller overshoot, better robustness, and smaller torque and stator flux ripples

Manuscript received March 20, 2018; revised June 26, 2018.

doi: 10.18178/ijeetc.7.3.108-113

compared with classical PI speed controller based DTC scheme.

II. SVM-DTC FOR IPMSM

A. Mathematical Model of IPMSM

The equations of the three-phase IPMSM in the α-β coordinate frame are shown as followings:

$$\begin{cases}\psi_\alpha = \int (u_\alpha - Ri_\alpha)dt \\ \psi_\beta = \int (u_\beta - Ri_\beta)dt\end{cases} \tag{1}$$

$$\psi_s = \sqrt{\psi_\alpha{}^2 + \psi_\beta{}^2} \tag{2}$$

$$T_e = \frac{3}{2} P_n (\psi_\alpha i_\beta - \psi_\beta i_\alpha) \tag{3}$$

where ψ_α, u_α, i_α represent the stator flux, stator voltage and stator current in α axis; ψ_β, u_β, i_β represent the stator flux, stator voltage and stator current in β axis; R is the stator resistance; P_n represents the pole pairs; T_e is the electromagnetic torque.

B. SVM-DTC

The basic principle of DTC is to select the optimal voltage vectors, which makes the stator flux linkage space vector rotates to required position while keeping magnitude within limited and generate desired torque [13]. It can regulate the stator flux and torque more precisely with fixed switching frequency when incorporating with SVM technique [6].

The simulation block of proposed adaptive NN-PI speed controller for SVM-DTC based IPMSM is shown in Fig. 1. The adaptive NN-PI speed controller uses the errors between reference speed and estimated speed as inputs to generate reference torque T_e^*. Then the torque PI regulator can produce reference angular θ of the stator flux linkage. At sampling time k, the flux amplitude $\psi_{s(k)}$ and phase angle $\theta(k)$ can be calculated from flux estimator. Then at next time k+1, they become $\psi_{s(k+1)}$ and $\theta(k+1)$ with $\Delta\theta$ between $\psi_{s(k)}$ and $\psi_{s(k+1)}$, as shown in Fig. 2 [7], [10]. If we define $\psi_{s(k+1)}$ as given stator flux ψ_s^*, $\psi_{s(k)} = \psi_s$, then we get (4).

$$\psi_{s(k+1)} = \begin{bmatrix}\psi_{\alpha(k+1)} \\ \psi_{\beta(k+1)}\end{bmatrix} = \begin{bmatrix}|\psi_s^*|\cos(\theta+\Delta\theta) \\ |\psi_s^*|\sin(\theta+\Delta\theta)\end{bmatrix}$$

$$\psi_{s(k)} = \begin{bmatrix}\psi_{\alpha(k)} \\ \psi_{\beta(k)}\end{bmatrix} = \begin{bmatrix}|\psi_s|\cos(\theta) \\ |\psi_s|\sin(\theta)\end{bmatrix} \tag{4}$$

From Fig. 2, we can get that the error vector of stator flux linkage as (5), also known as reference stator flux linkage vector. Afterward, the equivalent reference voltage space vectors U_{ref} and duration are selected and calculated according to ψ_{ref}, thus ψ_{ref} can be reduced to zero. Through the discretization of (1), the discretization $\psi_{ref} = u_{s(k)}T_s - Ri_{s(k)}T_s$ is obtained. T_s is the sampling interval. Then reference voltage vectors can be acquired as in (6).

$$\psi_{ref} = \begin{bmatrix}\psi_{\alpha ref} \\ \psi_{\beta ref}\end{bmatrix} = \begin{bmatrix}\psi_{\alpha(k+1)} - \psi_{\alpha(k)} \\ \psi_{\beta(k+1)} - \psi_{\beta(k)}\end{bmatrix} \tag{5}$$

$$U_{ref} = \begin{bmatrix}u_{\alpha ref} \\ u_{\beta ref}\end{bmatrix} = \begin{bmatrix}u_{\alpha(k)} \\ u_{\beta(k)}\end{bmatrix} = \begin{bmatrix}\psi_{\alpha ref}/T_s + Ri_{\alpha(k)} \\ \psi_{\beta ref}/T_s + Ri_{\beta(k)}\end{bmatrix} \tag{6}$$

Based on these reference voltage vectors, the SVPWM (space vector pulse width modulation) will select voltage vector, determine action time and control signals for inverter [10]. This adopted SVM-DTC still retains all the advantages of conventional DTC by replacing two hysteresis controllers with a torque PI regulator and Voltage Space Vector Reference (VSVR), the switching table with a SVM.

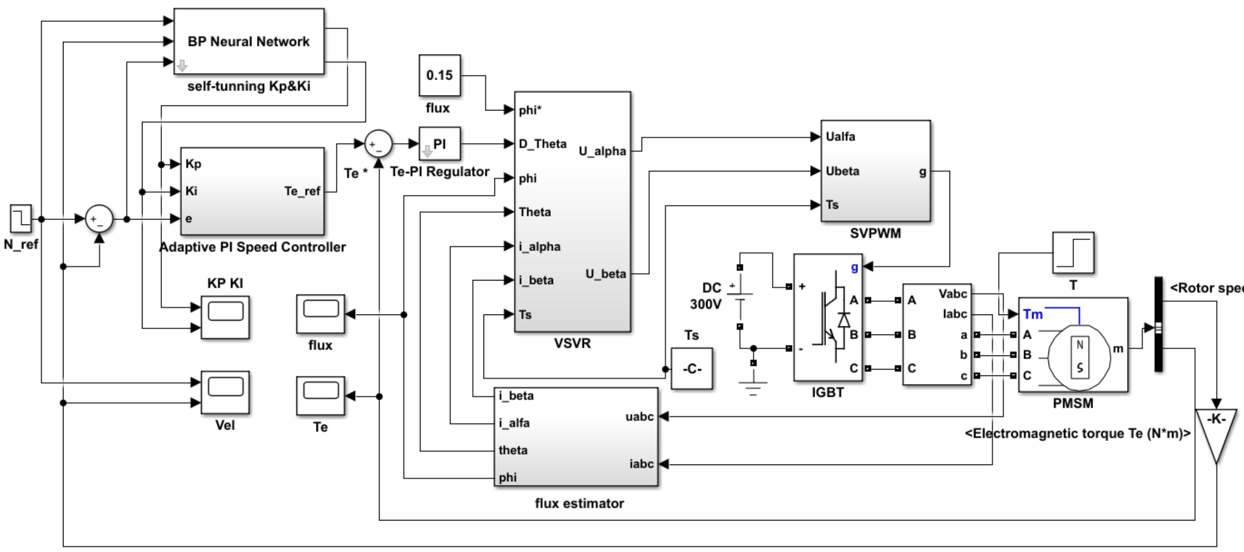

Figure 1. Simulation block of proposed control scheme.

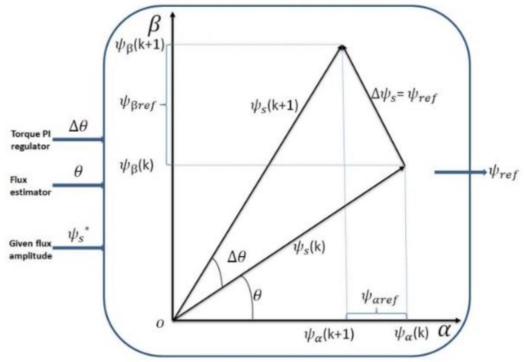

Figure 2. Signal flow chart of generating reference flux vector.

III. NEURAL NETWORK-PI SPEED CONTROLLER

Inspired by the marvellous function of neurons, the artificial neural network (ANN) has been developed very fast to solve big scale and complex problems recently. Numerous works [12], [15]-[18] have demonstrated that ANN is suitable for dynamic and nonlinear control systems due to the capability of processing, analyzing and learning. The speed controller of DTC structure is a nonlinear system, which has disturbances of load inertia and motor parameters variation against temperature [14]. This makes it difficult for PI speed controller to perform sufficiently well for this DTC control system. This paper proposes an adaptive speed controller based on back propagation (BP) neural network, which is verified by simulation with higher performances.

A. Incremental PI Controller

The PI control theory has been one of the most widely used methods in industrial application. In continuous-time, the PI equation is expressed in (7). When the sampling period is very small, a discrete-time PI controller can be obtained as (8) by replacing integrate with summation and replacing derivative with difference quotient of (7).

$$u(t) = k_p(e(t) + \frac{1}{T_i}\int_0^t e(\tau)d\tau) \tag{7}$$

$$u(k) = k_p(e(k) + \frac{T_s}{T_i}\sum_{j=0}^{k} e(j)) \tag{8}$$

where $u(t)$ and $u(k)$ are controller outputs at continuous-time t and discrete-time k, respectively; $e(t)$ and $e(k)$ represent tracking errors at continuous-time t and discrete-time k, respectively; k_p is proportional gain; T_i is integral time constant; T_s is the sampling period. For convenience of program coding work, (8) can be described as incremental form as (9) [16]:

$$\Delta u(k) = k_p\left(e(k) - e(k-1)\right) + k_i e(k) \tag{9}$$

where k_i is the integral parameter gain.

B. Structure of NN-PI Speed Controller

The NN-PI speed controller using error back propagation (BP) algorithm consists of two parts. One is classical PI controller which can regulate motor speed in the closed loop. The other is BP neural network which can tune the parameters of k_p and k_i online to achieve the optimal performance. The schematic structure of NN-PI speed controller is shown as in Fig. 3.

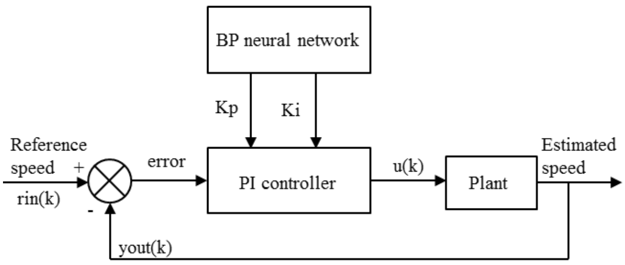

Figure 3. The structure of NN-PI speed controller.

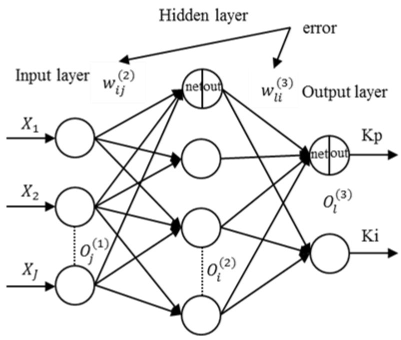

Figure 4. The structure of BP neural network.

The adopted BP neural network has three-layer, which is described as in Fig. 4. The numbers of neural nodes of input layer, hidden layer and output layer is J, I and 2, respectively. The inputs are the selected running states of system. The outputs are the parameters of PI controller.

As shown in Fig. 4, the neuron i of hidden layer at k can be expressed by following equations (10), (11):

$$o_i^{(2)}(k) = f\left(net_i^{(2)}(k)\right) \tag{10}$$

$$net_i^{(2)}(k) = \sum_{j=0}^{J} w_{ij}^{(2)} o_j^{(1)} \tag{11}$$

where $net_i^{(2)}(k)$ and $o_i^{(2)}(k)$ denote the input and output of neuron i, respectively; $w_{ij}^{(2)}$ denotes the connection weight parameter between jth and ith neurons; $o_j^{(1)}$ is the input the jth neuron; $f(x) = \tanh(x)$ is tangent hyperbolic activation function. Similarly, the output $O_l^{(3)}(k)$ and input $net_l^{(3)}(k)$ of output layer are given by (12), (13).

$$o_l^{(3)}(k) = g\left(net_l^{(3)}(k)\right) \quad l = 1, 2 \tag{12}$$

$$net_l^{(3)}(k) = \sum_{i=1}^{I} w_{li}^{(3)} O_i^{(2)} \tag{13}$$

where $g(x) = 0.5(1 + \tanh(x))$ is the activation function of output layer.

The weights are updated using gradient descent method based on BP algorithm, which is given by (14):

$$w(k) = -\eta \frac{\partial E(k)}{\partial w} + \alpha w(k-1) \tag{14}$$

where $E(k) = 0.5(rin(k) - yout(k))^2$ is cost function, η is learning rate, α is momentum rate. The weights updating equations are given as follows:

$$w_{li}^{(3)}(k) = \alpha w_{li}^{(3)}(k-1) + \eta \delta_l^{(3)} O_i^{(2)}(k) \tag{15}$$

$$w_{ij}^{(2)}(k) = \alpha w_{ij}^{(2)}(k-1) + \eta \delta_i^{(2)} O_j^{(1)}(k) \tag{16}$$

where

$$\delta_l^{(3)} = error(k) \frac{\partial y(k)}{\partial u(k)} \frac{\partial u(k)}{\partial O_l^{(3)}(k)} g'\left(net_l^{(3)}(k)\right)$$

$$\delta_i^{(2)} = f'\left(net_i^{(2)}(k)\right) \sum_{l=1}^{2} \delta_l^{(3)} w_{li}^{(3)}(k).$$

IV. Simulation and Results

The proposed method is evaluated by simulation on MATLAB. The parameters of IPMSM drive system considered in this study are listed in Table I.

To demonstrate the effectiveness of the presented NN-PI speed controller, the simulation results for a classical PI speed controller and the NN-PI speed controller are compared. The simulation model of proposed method is shown in Fig. 1. Both of the methods are tested under same conditions with reference speed, load torque reference and simulation settings.

TABLE I: Parameters of IPMSM

Parameter	**Values**
Number of pole pairs p_n	4
Stator resistance R	1.2Ω
Magnet flux linkage	0.175Wb
d-axis inductance L_d	4.4mH
q-axis inductance L_q	6.4mH
Moment inertia J	0.0008 kgm^2
Viscous friction F	0.0001 (N·m·s)

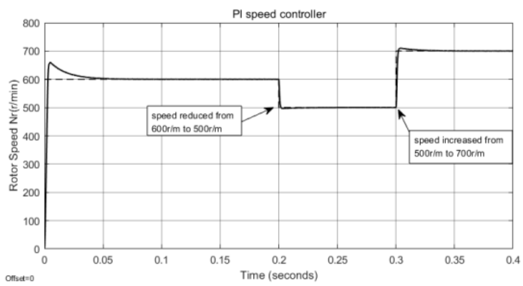

(a)

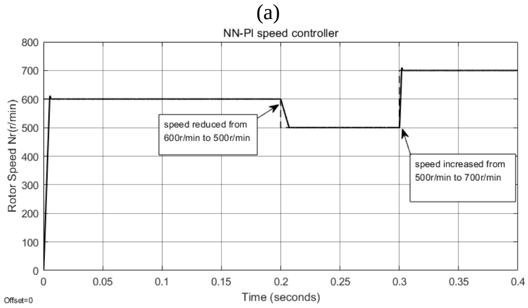

(b)

Figure 5. Simulation results of speed tracking performances at speed changes (a) PI speed controller; (b) NN-PI speed controller.

The dynamic responses of PI and NN-PI speed controllers are investigated by subjecting the IPMSM drives to a variable speed operation. Simulation is started at the speed 600 r/min with a sudden speed reduction to 500 r/min at 0.2s and a sudden speed increase to 700 r/min at 0.3s. Fig. 5 shows the simulation results of two techniques. Obviously, the proposed NN-PI speed controller technique can obtain much better dynamic performance to speed change with smaller speed overshoot and faster speed transient response. Fig. 6 shows the adaptive PI parameters k_p and k_i tuned by neural network. It can be clearly observed that the k_p and k_i will be tuned continuously until the motor tracks the reference speed. It means the proposed NN-PI speed controller could have optimal parameters at most simulation period.

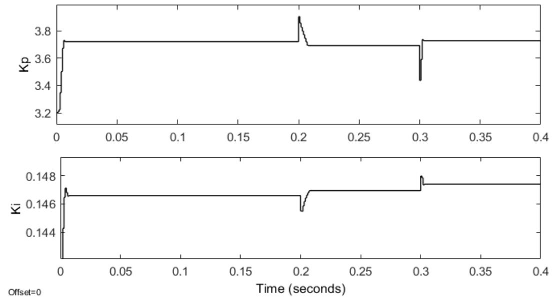

Figure 6. Tuned parameters k_p and k_i of NN-PI speed controller.

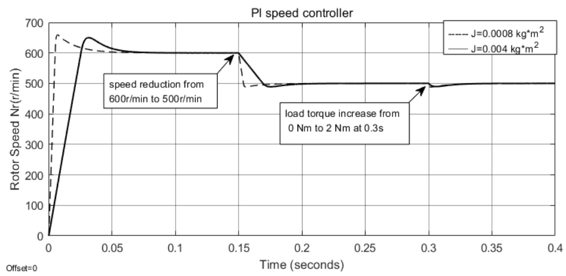

(a)

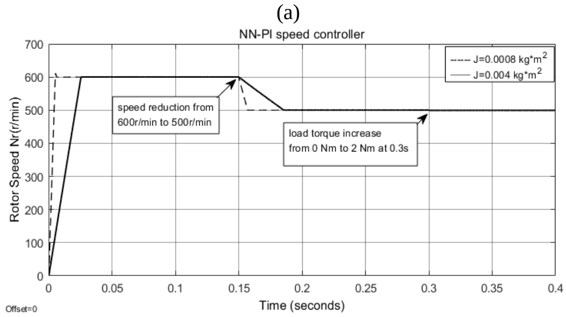

(b)

Figure 7. Simulation results of speed tracking performances at inertia and load torque changes (a) PI speed controller; (b) NN-PI speed controller.

Fig. 7 shows the speed tracking performances of the proposed NN-PI speed controller and conventional PI speed controller under the parameter uncertainties when the inertia coefficient increases from 0.0008 kgm^2 to 0.004 kgm^2 and load torque suddenly increases from 0 Nm to 2 Nm at 0.3s. As shown, both of them need longer time to track reference speed when system inertia increases. It's reasonable since inertia can influence the speed rate of motor as (17). Compared to PI speed controller, the proposed method still can achieve much better results with short setting time and much smaller speed overshoots when inertia and load torque change.

$$\frac{dw_m}{dt} = \frac{1}{J}\left(T_e - Fw_m - T_m\right) \tag{17}$$

where w_m is mechanical angular speed of motor and T_m is load torque.

It's clearly shown that the proposed method obtains great improvement in reduction of overshoot at the start-up period. Moreover, NN-PI speed controller has much better speed tracking performances than PI controller when facing load torque variations and sudden speed change.

Finally, we compare the estimated electromagnetic torque and stator flux magnitude responses between PI speed controller and proposed NN-PI speed controller for SVM-DTC system under the same operating condition. As can be seen from Fig. 8 and Fig. 9, both of them can obtain excellent results with small torque and flux ripples, as about 0.2Nm and 0.001Wb, respectively. From Fig. 8, it's observed that proposed method has relatively better performance with lower pulse and faster dynamic response in start-up period. Moreover, NN-PI can also perform more stable under sudden load torque variation and speed reduction.

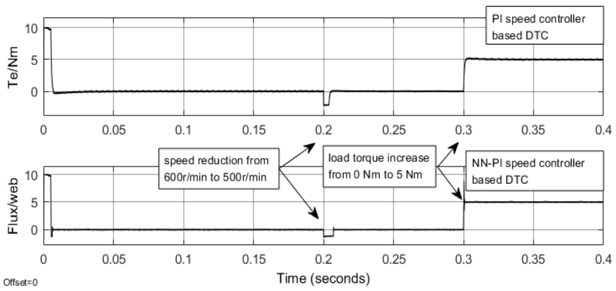

Figure 8. The comparison of estimated torque between PI and NN-PI speed controller for SVM-DTC system.

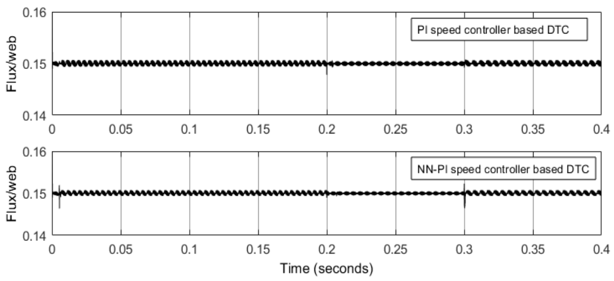

Figure 9. The comparison of stator flux between PI and NN-PI speed controller for SVM-DTC system.

V. Conclutions

In this research, an online trained NN-PI speed controller using BP algorithm for SVM-DTC technique based IPMSM drives is developed and implemented. BP neural network is applied to tune parameters k_p and k_i of PI speed controller, which overcomes the disadvantages of conventional PI controller with high dependence on controlled model and time-consuming tuning work.

The simulation results demonstrate the effectiveness of the proposed NN-PI speed controller with faster response, much smaller overshoot and better robustness in speed tracking under reference speed changes, inertia increases and load torque variation. Furthermore, SVM-DTC technique with proposed method can achieve good torque and flux performances with small ripples.

Acknowledgment

The research was supported by the Industry Core Technology Development Project "Development of 2kW/kg, 100kW class IPMSM electric drive system with high efficiency cooling" through the Ministry of Trade, Industry and Energy (Grant Number : 10063006).

References

[1] K. Song and W. G. Liu, "Permanent magnet synchronous motor field oriented control and HIL simulation," in *Proc. IEEE Vehicle Power and Propulsion Conference*, Harbin, 2008, pp. 4-6.

[2] C. Xia, S. Wang, X. Gu, Y. Yan, and T. Shi, "Direct torque control for VSI-PMSM using vector evaluation factor table," *IEEE Trans. Ind. Electron.*, vol. 63, no. 7, pp. 4571-4583, July 2016.

[3] A. Haddoun, M. E. H Benbouzid, D. Diallo, R. Abdessemed, J. Ghouili, and K. Srairi, "A loss-minimization DTC scheme for EV induction motors," *IEEE Trans. Veh. Technol.*, vol. 56, no. 1, pp. 81–88, Jan. 2007.

[4] I. Takahashi and T. Noguchi, "A new quick-response and high-efficiency control strategy of an induction motor," in *Conf. Rec. IEEE IAS Annu. Meeting*, 1985, pp. 1665-1675.

[5] Q. Liu and K. Hameyer, "Torque ripple minimization for direct torque control of pmsm with modified fcsmpc," *IEEE Trans. Ind. Appl.*, vol. 52, no. 6, pp. 4855–4864, Nov./Dec. 2016.

[6] Y. Choi, H. Choi, and J. Jung, "Feedback linearization direct torque control with reduced torque and flux ripples for IPMSM drives," *IEEE Trans. Power Electron.*, vol. 31, no. 5, pp. 3728-3737, May. 2016.

[7] L. Tang, L. Zhong, M. F. Rahman, and Y. Hu, "A novel direct torque controlled interior permanent magnet synchronous machine drive with low ripple in flux and torque and fixed switching frequency," *IEEE Trans. Power Electron.*, vol. 19, no. 2, pp. 346–354, Mar. 2004.

[8] C. A. Martins, X. Roboam, T. A. Meynard, and A. S. Carvalho, "Switching frequency imposition and ripple reduction in DTC drives by using a multilevel converter," *IEEE Trans. Power Electron.*, vol. 17, no. 2, pp. 286–297, Jan. 2002.

[9] Y. Cho, K. B. Lee, J. H. Song, and Y. I. Lee, "Torque-ripple minimization and fast dynamic scheme for torque predictive control of permanent magnet synchronous motors," *IEEE Trans. Power Electron.*, vol. 30, no. 4, pp. 2182–2190, Apr. 2015.

[10] X. Wang, Y. Xing, Z. He, and Y. Liu, "Research and Simulation of DTC Based on SVPWM of PMSM," in *Proc. International Workshop on Information and Electronics Engineering*, vol. 29; pp. 1685–1689, 2012.

[11] Y. Su, C. Zheng, and B. Duan, "Automatic disturbances rejection controller for precise motion control of permanent-magnet synchronous motors," *IEEE Trans. Ind. Electron.*, vol. 52, no. 3, pp. 814–823, Jun. 2005.

[12] T. Pajchrowski, K. Zawirski, and K. Nowopolski, "Neural speed controller trained online by means of modified RPROP algorithm," *IEEE Trans. Ind. Informat.*, vol. 11, no. 2, pp. 560–568, Apr. 2015.

[13] F. Hamidia, M. S. Boucherit, A. Larabi, and M. Bouhedda, "Direct torque control with ANN speed controller based on kalman filter for PMAM," in *Proc. IEEE Trans, 9th International Conference on Systems, Signals and Devices*, 2012.

[14] S. Li and Z. Liu, "Adaptive speed control for permanent magnet synchronous motor system with variations of load inertia," *IEEE Trans. Ind. Electron.*, vol. 56, no. 8, pp. 3050–3059, Aug. 2009.

[15] H. Ji and Z. Li, "Design of neural network PID controller based on brushless DC motor," in *Proc. Second International Conference on Intelligent Computation Technology and Automation*, vol. 3, pp. 46-49, 2009.

[16] X. Fu and S. Li, ''A novel neural network vector control technique for induction motor drive,'' *IEEE Trans. Energy Convers.*, vol. 30, no. 4, pp. 1428–1437, Dec. 2015.
[17] S. Omatu, M. Yoshioka, T. Kosaka, and H. Yanagimoto, "Neuro-PID control of speed and torque of electric vehicle," *International Journal on Advances in Systems and Measurements*, vol. 3, no. 1–2, 2010.
[18] J. Kang, W. J. Meng, A. Abraham, and H. B. Liu, "An adaptive PID neural network for complex nonlinear system," *Neurocomputing*, vol. 135, pp. 79–85, 2014.

Zhenyu Jia received the B.S. degree in Mechanical Engneering from Shanghai University of Technology and Science, Shanghai, China, in 2014. He is currently working towards the M.S. degree in the School of Electrical Engineering, University of Ulsan, Ulsan, South Korea. His research interests includes intelligent control, electric machine drives and direct torque control technique.

Byeongwoo Kim received received the B.E, M.E. and Ph.D. degree in Precision Mechanical Engineering from Hanyang University, South Korea. He worked at KOSAKA Research Center in 1989. He worked at KATECH electrical technology Research Center from 1994 to 2006. His current research interests include advanced driving assistance system (ADAS), and autonomous emergency braking (AEB) system.